International Forum on Aeroelasticity and Structural Dynamics
IFASD 2017
25-28 June 2017, Como - Italy

FUEL LOADS IN LARGE CIVIL AIRPLANES

Francesco Gambioli[1] and Arnaud George Malan[2]

[1]Airbus in the UK
Pegasus House, Aerospace Avenue, Filton Bristol (UK) BS34 7PA
francesco.gambioli@airbus.com

[2]University of Cape Town
Cape Town, South Africa, 7701
arnaud.malan@uct.ac.za

Keywords: Sloshing, Fuel, Pressure, Loads.

Abstract: The research on fuel loads at the Airbus Loads department will be put in context with the broader view and needs of the aerospace sloshing community.

The application of a novel methodology for free surface modeling, developed in partnership with the University of Cape Town will be presented. An overview of the "Validation and Verification" process undergone by the method will be shown, with comparison of numerical simulation and experimental results.

Further analysis of dynamic loads on the walls of fuel containers will be discussed for certain cases of interest for large aircraft. The industrial applications of a Reduced Order Model (ROM) developed to cover the design space of the fuel tanks will also be presented.

1 INTRODUCTION

The modelling of fluid free surface in containers is of interests in various fields of the aerospace industry.

For modern satellites, the design is often driven towards lightweight structures, high pointing accuracy and long life expectations, ref. [1]. These can results in relatively large proportion of the overall weight being allocated to the liquid propellant. Typical aerospace launchers also have a high ratio of payload to propellant mass (~20:1 for the European Arianne 6, ref [2]).

Therefore the movement of the liquid fuel within its containers can significantly affect the dynamics of these systems, during in-orbit controlled manoeuvers and atmospheric gust encounters in the launch phase. Extensive analysis of the environment and the modelling for space applications is provided in ref. [3]-[5].

In the field of aircraft design, the study of fuel movement within tanks is of paramount importance for the design of the fuel management control system, the evaluation of the handling characteristics of the aircraft and ultimately the assessment of the structural integrity of the containment structure. Other specialized applications are related to transport of non-flammable liquids, such as water, for firefighting purposes (ref. [6]).

This paper focuses on the research carried out at the Airbus Loads department, in Filton, UK. The primary aim of this work has been the definition of the loads to be used for the structural design of wing fuel tanks.

In course of the last decade, two methods, namely the Smooth Particle Hydrodynamics or SPH (ref. [7], [8]) and Volume of Fluids or VOF (ref. [9], [10]), have been investigated in details to assess their capabilities for modelling the particular design environment of the civil aircraft. These are "large" transport airplanes, subject to CS25 type certification, ref. [11], where most of the fuel (~30% of the overall mass at take-off) is stored in the wing tanks. The operational environment of such aircraft includes highly dynamic events such as gust encounters and landing impacts, which can excite the structural flexibility of the airframe and therefore result in high accelerations (15~20g) at a wide range of frequencies (0-25Hz).

The flexible wing response to dynamic loading is such that, to the authors' knowledge, no extensive literature is available to describe comprehensively the flow regimes in a tank subject to rapidly varying accelerations perpendicular to the free surface.

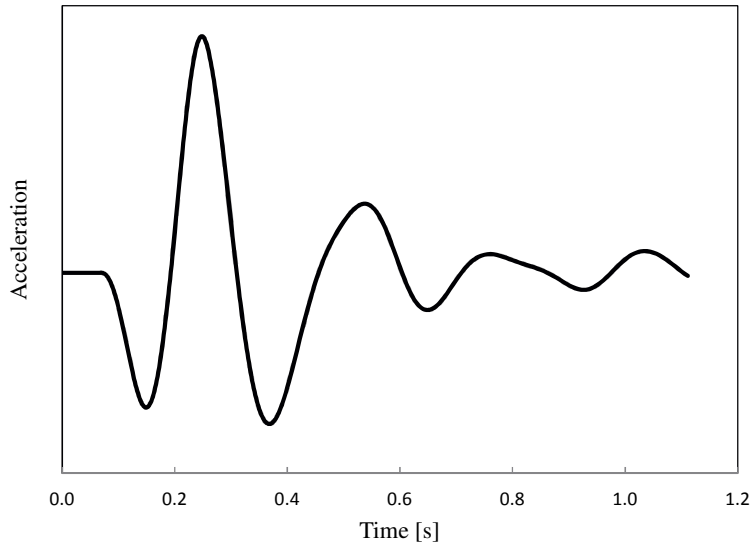

Figure 1: Typical Vertical Acceleration of Wing Tank

Figure 1 shows the typical acceleration response of a wing subject to discrete gust loading as per CS25.341 (ref. [11]). The acceleration scale is not shown in the graph, however the amplitude of the peak accelerations for design cases can go beyond gravity and therefore lead to the fuel leaving the bottom of the tank and impacting the tank roof.

While in space applications the sudden deceleration at the separation of a launcher stage can lead to severe impact forces, these are generally resolved to a single event as opposed to the cyclic wing oscillations which are repetitive in nature. Another peculiarity of the wing tanks is their geometry, which is not that of a solid of revolution, and the presence of several baffles (ribs) affects significantly the dynamics of the fuel in the direction parallel to the free surface.

Due to the uniqueness of the conditions described, and consequent lack of data available in literature, an experimental campaign is deemed necessary to investigate the characteristics of the fluid flows in wing tanks, for the subsequent validation and verification of numerical results derived from the SPH and VoF methods (ref [12]).

Following its verification, the VoF method has been chosen and used to derive a set of design rules for the calculation of the tank wall pressures. These proved to be less conservative than past practices and can be used for the local sizing of the wing box structures.

2 AIRCRAFT LOADS CALCULATION

2.1 Aircraft Loads Model

The aeroelastic model used for loads calculation and analysis includes representations of the aircraft aerodynamic, inertial and elastic characteristics and is also coupled in closed loop with the electronic flight control system.

The model is used to simulate the aircraft responses to the environmental (gust, ground impact, etc.) and pilot (maneuvers) inputs, which result in loads at discrete points on the airframe. The outputs are a series of time histories which defined the state of the flexible aircraft under external loading. Each state, at a given point in time, is by definition a balanced load case.

The requirement to cover the complete flight envelope, in terms of aircraft speed and altitude, and all the practical mass distributions, in terms of payload and fuel on board, leads to thousands of possible combinations; therefore part of the loads activity focuses on "reducing" the complexity of the model (through rational reduction of the degrees of freedom in the Finite Element Model of the structure for example), while maintaining the level of accuracy needed for selecting the critical design load cases.

Due to the reduced complexity, the loads model representation is too coarse for specific component design, i.e. total forces on wing box sections are available rather than the corresponding pressure distributions. Therefore a mapping exercise is necessary to achieve the level of detail required for local sizing. A schematic representation of the process is shown in Figure 2.

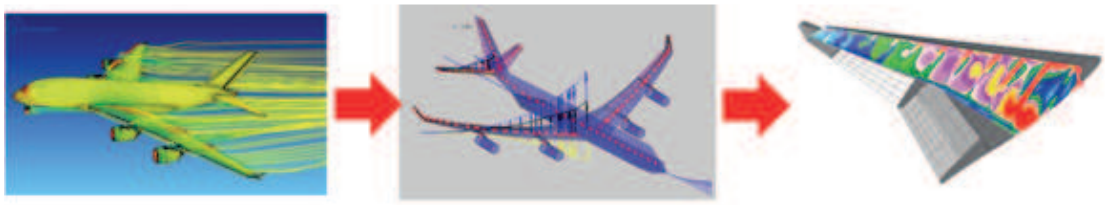

Figure 2: Loads Calculation Process

2.2 Fuel Pressure Calculation

Fuel pressures are calculated as part of the post-processing, or mapping, of the loads model results. This uses input quantities calculated for each load case, e.g. wing accelerations and deflections.

The actual pressure values are computed using the hydrostatic law:

$$p_s = \rho \, N_g \, h \tag{1}$$

Where p_s is the pressure at any given point in the tank, ρ is the fuel density, N_g is the acceleration of the tank, and h is the distance between the fuel free surface and the point of interest.

The usage of equation (1) has two limitations:

- The calculated fuel loads are static head pressures, therefore they do not account for any dynamic effects due to the fuel movement within the tanks.
- The selection of fuel pressure design cases is based on maximum acceleration values, which inherently do not account for the effect of the fuel movements.

To overcome the shortfalls in the load calculation and selection processes, the current methodology prescribes the application of dynamic amplification factors as per equation (2).

$$p_d = DAF\ p_s \tag{2}$$

Where p_d is the design pressure and DAF is a dynamic amplification factor greater or equal to one. In practice the amplification factor is applied by artificially increasing the fuel head so to have a full volume even for conditions in which the tanks are only partially filled. This avoids unnecessary conservatism for full tank cases (with no dynamic effects), as the amplification automatically reduces to one.

Traditionally this approach has proved to be safe, conservative, is accepted by the certification authorities and is consistent with what prescribed by EASA CS-25 (ref. [11]) to calculate fuel pressure loads in highly dynamic events such as survivable crash landings.

3 EXPERIMENTAL CAMPAIGN

As mentioned in section 1, a series of physical tests has been performed for validation and verification of numerical predictions. The tests are defined in terms of acceleration time histories, derived from a survey of loads simulation results and a set of prescribed cases. These are applied to a scaled tank model at the Bristol University Earthquake Simulator facility. The fluid used in the test is water. Potassium permanganate is used as a coloring agent to ensure water visibility. The pressures occurring within a tank filled to either 25% or 75% volume levels are measured.

3.1 Test Specimen Geometry

The size of the test specimen is based on the typical geometry of wing tanks.
All dimensions are given in aircraft axes, defined as follows:

- x is parallel to the wing chord
- y is parallel to the wing span
- z is perpendicular the plane of x and y (vertical).

Ratio	Typical Value
x/y	~4
y/z	~2

Table 1: Tank Dimension Ratios

The dimensions of the tank are then defined on the basis of the largest that could be accommodated by the Bristol University test facility. The resulting tank geometry is shown in Figure 3.

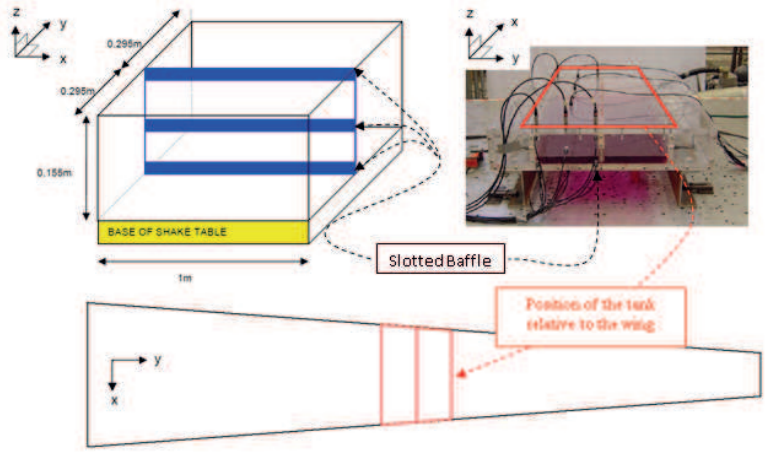

Figure 3: Test Specimen Geometry

The tank layout is representative of two wing box bays separated by an intermediate rib, which acts as a baffle. The baffle is further divided into two sections parallel to the x/z plane and bolted on either end to the tank sidewalls (parallel to the x/z plane), resulting in three slots of 12, 8 and 2mm respectively at the bottom, middle and top of the tank. This configuration mimics the actual wing design, where fuel can flow through intermediate ribs.

3.2 Test Case Definitions

The time-varying accelerations used for the tests are either derived from surveying the results of loads simulations or prescribed as cases of particular interest. The time signals can be classified in terms of amplitude and frequency of the oscillation, which are depended on type of loading condition considered.

For *Maneuvers*, which simulate the aircraft response to a pilot action, the loads model is quasi-static. These simulations include vertical, rolling and yawing maneuvers. The resulting time histories have low-frequency content (rigid body motion) and the amplitude of the oscillation does not exceed the static limit load-factor defined in ref. [11].

Ground cases simulate the loads introduced into the airframe through contact with the ground. Of particular importance for fuel pressure calculation are loads due to dynamic landing impact. The loads model is fully dynamic for these cases and the wings can oscillate significantly for the outermost tanks. The frequency spectra of the time histories in this category present a high-frequency content (flexible modes are excited) and the amplitude of the oscillation can be significantly higher than in the maneuvers.

Discrete Gust cases simulate the encounter of a sinusoidal-shaped gust. The gust input is tuned to the dimensions of the specific aircraft under analysis. Once again the loads model is fully dynamic for these cases; the characteristics of the time signal are comparable with the ground cases.

Continuous Turbulence simulates the loads on the airframe due to atmospheric turbulence. The frequency content of the excitation is prescribed in the certification specifications. The corresponding tests are defined as time histories with the same frequency spectrum of the original input. As for discrete gust, the loads model used is fully dynamic.

In addition to loads-model derived time histories, a series of test cases has been designed to explore the behavior of the fluid in under particular excitations, with the potential to result in significant loads on the tank walls.

Harmonic oscillations are also defined to analyze the behavior of the fuel at the frequencies of the first wing bending and wing fore/aft modes. These tests are designed to assess the influence of the structural characteristics of the wing on the fuel motion. Additional harmonic oscillation tests are defined to excite the sloshing frequency of the fluid, so to investigate the maximum natural response of the fluid. For a rectangular tank at a given fill level, the sloshing frequency can be determined following the approaches described in [3]-[5].

Finally repetitive impulsive accelerations are prescribed, to represent abrupt maneuvers and the consequent sudden acceleration of the tank. The time signal for these test cases is saw-tooth acceleration between 0 to 2.5g in the three directions (x, y and z). The time to reach to maximum acceleration is dictated by the specifications of the test rig.

3.3 Scaling Laws and Time History Manipulation

Since testing of a full-scale aircraft wing is not practical, the acceleration inputs need to be scaled to represent the required physical conditions. For the harmonic oscillations the scaling law proposed in [13] is used to design the experiments, based on the Froude rule, as follows:

$$V_m = V_f \, \lambda^{1/2} \tag{3}$$

$$T_m = T_f \, \lambda^{1/2} \tag{4}$$

Where V and T represent the instantaneous velocity and the period of oscillation respectively; the subscripts m and f indicate the model and full scale and λ is the ratio of model length over full scale.

Equation (3) guarantees that the full scale Froud number is preserved in the laboratory test, Equation (4) is based on the classical derivation natural frequency for the linear sloshing case (ref. [3]-[5]) and ensures similitude in terms of sloshing frequencies. With this scaling, the gross liquid surface shape at any instant in time is reproduced if liquid inertia and gravity forces are dominant. The velocities in the model are smaller and the frequencies of the sloshing are higher.

For tests defined as complete time history resulting from the loads model, scaling is required due to the limit of maximum acceleration and displacement achievable by the test rig. The required accelerations are achieved at reduced displacement by summation to a constant acceleration term, resulting in a modified time history with the same time-derivative of the original signal.

Figure 4 gives some examples traces of displacement time histories for the first 1.2s in the directions perpendicular to the baffle (y) and to the free surface (z).

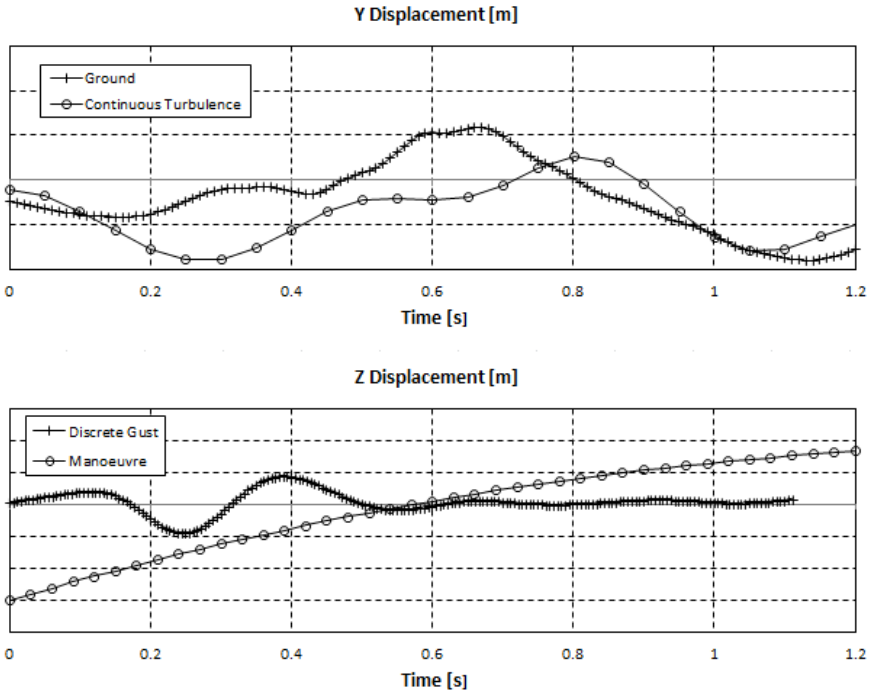

Figure 4: Displacement Time Histories

3.4 Experimental Apparatus and Sensors

The Bristol University shake table is a 6-axis Earthquake Simulator which consists of a 3m x 3m cast aluminum platform weighing 3.8 tonnes. The platform has the shape of an inverted pyramid made from four sections and has a honeycomb-like network of stiffening diaphragms giving it high strength and bending stiffness.

A total of three SETRA type 141A accelerometers are used. The accelerometers have a calibrated range of +/-8g that is traceable to UK national standards. 36 DRUCK PDCR81 1 bar pressure sensors are used to monitor the pressures within the tank. These sensors are installed within holes tapped through the tank walls. Their sensing faces are flush with the internal walls of the tank. Protection tape is used to prevent water escaping from around the sensors. The transducers are positioned across the surface of one of the bays of the tank: nine on the roof - nine on the floor - five on the baffle, five on the sidewall opposite to the baffle, three on each of the remaining walls. A high speed PHOTRON SA1 digital video camera operating at 250 frames per second is used to create digital video files of each test.

3.5 Data Processing

The experimental pressure data is analyzed in details in ref. [14], while some additional aspects discussed in ref. [15].

Ref. [14] confirms the repeatability of the test cases, their bi-dimensional nature (with the exception of those defined by three-component accelerations) and also provides a procedure for data processing.

Figure 5 shows the effect of the processing on the raw experimental data:

1) Butterworth (low pass) filter is applied to remove noise
2) Initial (time equal zero) pressures are calibrated to hydrostatic pressure
3) Shifting is applied to time correlate the results.

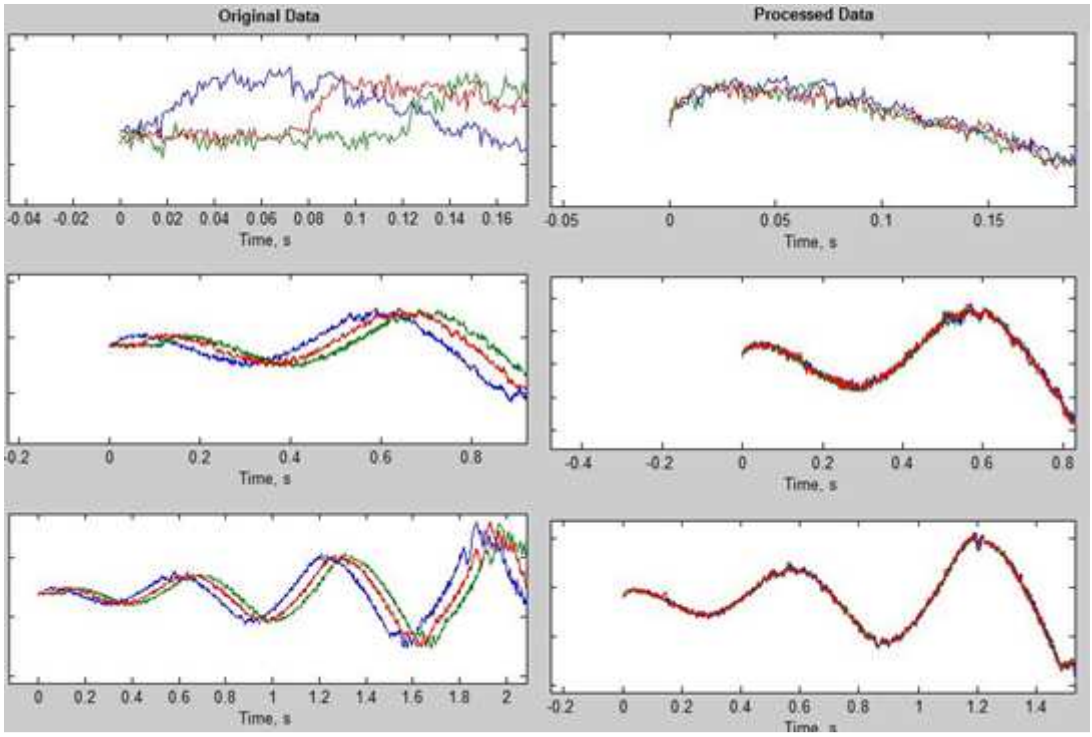

Figure 5: Data Processing

After processing, good repeatability is observed in all the test cases analyzed in ref. [14].

4 NUMERICAL METHOD EVALUATION

4.1 Smooth Particle Hydrodynamics (SPH)

An overview of SPH and several of its applications can be found in ref. [16]. The method is Lagrangian in nature, mesh-free and capable of dealing with large deformations. Particles in the domain carry the properties of the fluid, which can be approximated using equation (5).

$$f(\boldsymbol{x}) \simeq \sum_i m_i \frac{f_i}{\rho_i} W(|\boldsymbol{x} - \boldsymbol{x_i}|, h) \tag{5}$$

Where f is any fluid property (such as density, velocity, pressure), $\boldsymbol{x}$ are geometrical coordinates, m and ρ are the mass and density of a particle respectively, the subscript i indicates a particle, W is the kernel function and h is the smoothing length of the kernel.

The approximation in equation (5) has the property of transferring spatial derivatives of the fluid property onto the kernel function, which is chosen to be non-zero only in the region within the smoothing length h. Once the spatial integration scheme is defined, the hydrodynamic problem reduces to a system of ordinary differential equations, which can be solved with standard time-stepping algorithms.

Because the approximation in (5) does not possess the property of interpolating the function at the boundary of the domain, no-slip boundary conditions are not naturally implemented in the SPH formulation.

Various methods are available in literature to represent solid boundaries in SPH:

- Ghost (or image) particles: at each time step additional particles are generated as mirrored images of the particles in proximity of the boundary. The density, velocity and pressure of those particles are assigned so to achieve reflection at the boundary. This method is difficult to implement in case of complex three-dimensional geometries.
- Bounce back: solid boundaries are represented by a layer of stationary or moving particles, whenever fluid particles cross the solid boundary are simply reflected back into the computational domain. Also this method can be difficult to generalize to complex three-dimensional problems.
- Boundary particles and forces: similarly to the bounce-back method the solid boundary is represented by a layer of stationary or moving particles. However these exert short range repulsive force, which are empirically assigned depending on the nature of the problem. Although this method is suited for modelling complex geometries, it can lead to the overall momentum of the fluid not being preserved.

Other methods are being or have been developed; see ref. [17] as an example, and the boundary condition implementation is a field of major research interest in SPH.

4.1.1 Numerical Simulations

The results presented in this section have been derived by BAE-Systems in ref. [18] using the BAESPH code; and some preliminary observations on the results have already been published in ref. [12]. The code implements boundary conditions with particles and forces of the Lenard-Jones type (as per ref. [18]).

Three test cases are presented: Sloshing frequency, a Manoeuver load case and a Gust load case. For the sloshing frequency case the acceleration of the tank is applied so to excite the first sloshing mode of the liquid at 25% fill level.

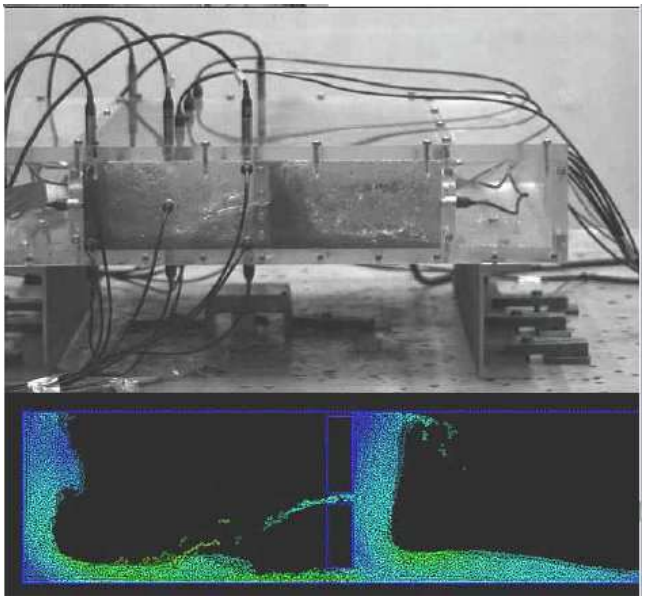

Figure 6: Sloshing Frequency – Flow Features

Figure 6 shows a comparison between the flow characteristics of the experimental test and the corresponding SPH numerical simulation. A representative time frame is chosen with the first 1000ms of the test/simulation. The SPH particles are colored for flow velocity.

It can be seen that the main flow features are well capture by the numerical simulation, in particular:

- The jet in the baffle slot
- The breaking of the rolling waves against the tank walls
- The interaction with waves with the tank roof.

Similar comparisons are given in ref. Figure 7 and Figure 8 for the maneuver and gust test cases, both at 25% fill level. In the maneuver case, tank acceleration is applied parallel to the baffle and the free surface, at relatively low frequency. Again the SPH is capable of modelling the free surface and the wave front motions with good accuracy.

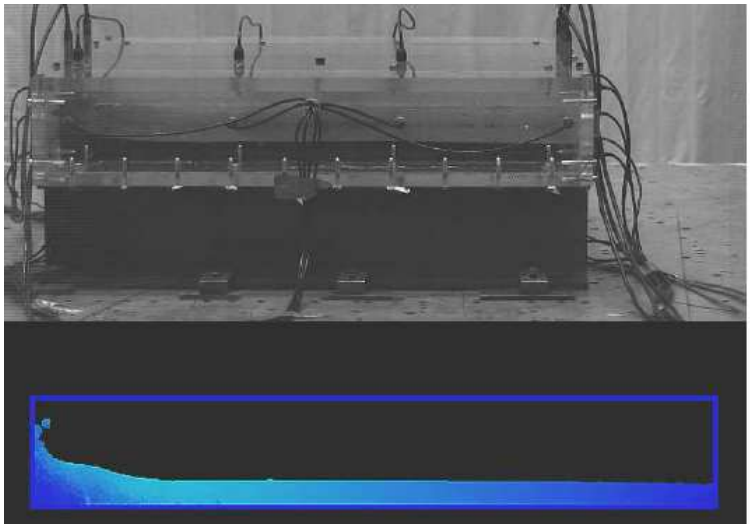

Figure 7: Maneuver Case – Flow Features

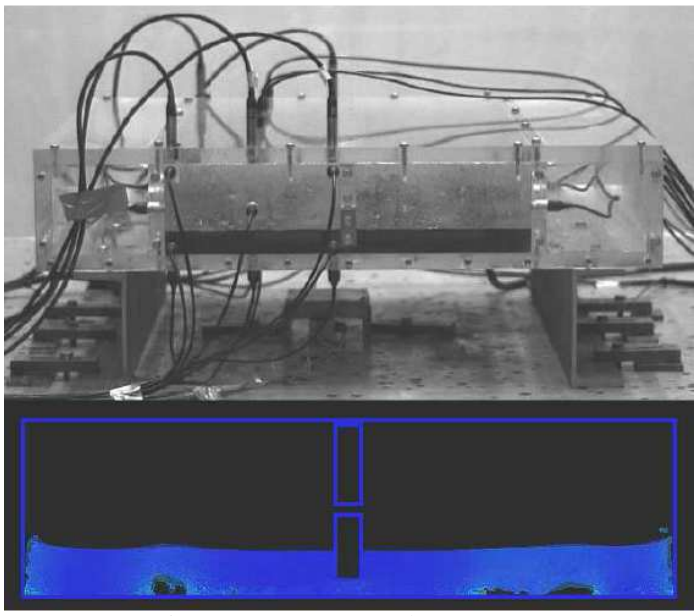

Figure 8: Gust Case – Flow Features

Finally the gust case is presented. Tank acceleration is applied perpendicular to the free surface, as to reproduce a vertical gust encounter. It can be noticed that areas of void (cavitation) start to form at the bottom of the tank, which do not appear in the experimental test.

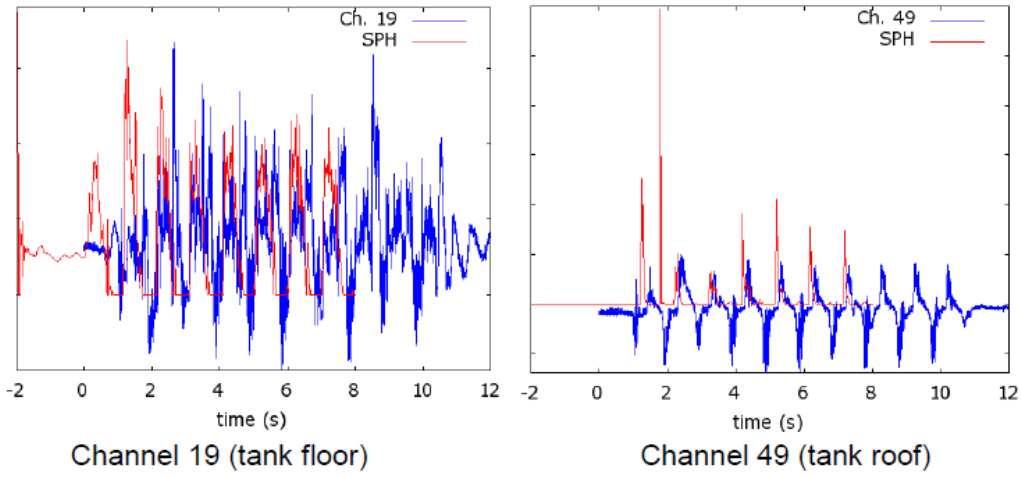

Figure 9: Sloshing Frequency – Floor and Roof Pressures

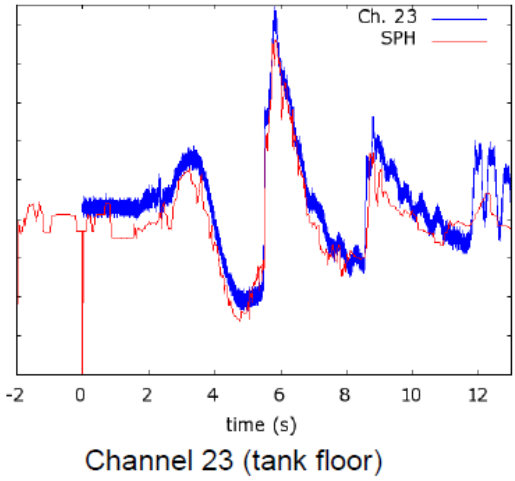

Figure 10: Maneuver Case – Floor Pressure

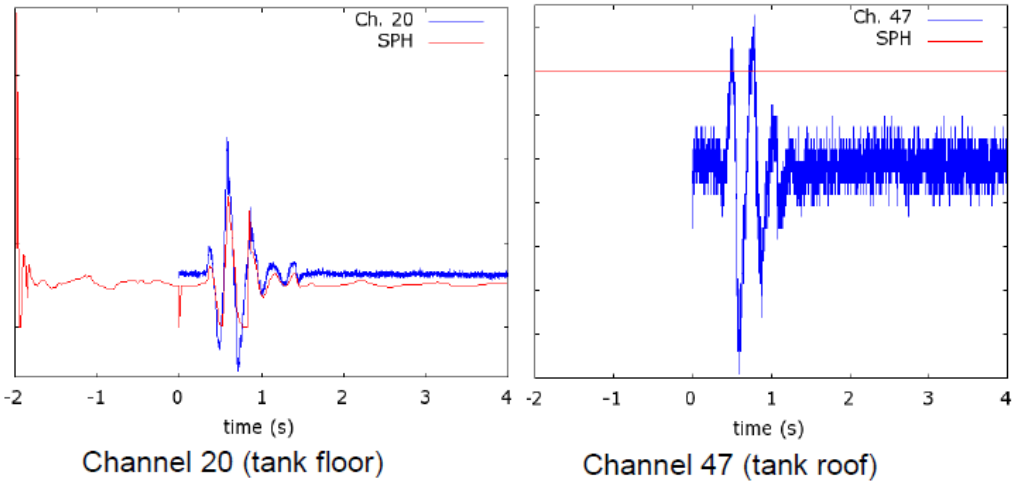

Figure 11: Gust Case – Floor and Roof Pressures

Figure 9, Figure 10 and Figure 11 depict the pressure comparisons between the experimental measurements and SPH simulations for the three test cases analyzed. Time starts at -2s for the SPH simulations to allow particle settling time, which is considered best practice when Lenard-Jones boundary conditions are used. For the maneuver case almost no variation in time is observed for roof pressure, therefore only floor pressure is shown in Figure 10. It

should be noticed that no processing is applied to the raw experimental data for calibration with hydrostatic pressure.

At the tank floor, the SPH results are in good agreement with the measurements for the gust and maneuver cases. However for the sloshing frequency case, even though the order of magnitude of the overall peak pressure is comparable, significant differences in the SPH time response is observed and the experimental data exhibits a phase lag compared to the numerical simulation.

At the tank roof, only positive increases in pressure (no suction) are seen from the SPH simulation of the sloshing frequency case and no time fluctuations are observed in the SPH results for the gust case. A very isolated and sharp pressure peak is given by SPH in the sloshing frequency case, which does not correlate with the experimental data.

The main discrepancies identified in the flow features and pressure data comparisons, namely the phase shift in the time response, the significant differences in the pressure time histories at the top and the formation of the voids due to cavitation at the bottom of tank, are all attributed to the single phase nature of the SPH simulations.

In fact it is inferred that the presence of air within the sealed tank:

- Has a damping effect on the sloshing oscillation of the liquid, so to cause the observed phase shift,
- Affects significantly the pressures at top of the tank, so that pressure (or suction) is observed when the air is pushed towards or away from the wall by the inertia of the liquid,
- Cushions the vertical movement of the fluid, so to provide resistance to the liquid departing from the tank bottom (piston-like effect).

The nature of the sharp pressure peak at the tank roof in Figure 9 is not analyzed in details, but it is thought to be an artefact of the implementation of solid boundary condition using Lenard-Jones repulsive forces. When isolated particles approach the tank wall with relative high speed, they can potentially reach a zone where the boundary forces are extremely high, resulting in unphysically high pressures.

It is of interest to notice that the limitation of single phase is not inherent to the SPH method; however the additional particles required to model the air flow would inevitably increase the computational cost of the method, generally regarded as one of its main advantages over more traditional mesh formulations.

Following from the validation exercise, SPH is regarded as a valuable mean to understand the qualitative nature of the flow field within large aircraft fuel tanks. However the issues encountered in the pressure predictions prompted the authors to investigate other options, and in particular the Volume of Fluid method.

4.2 Volume of Fluid (VoF)

Volume of Fluid (VoF) is a free-surface modelling technique, belonging to the class of Eulerian methods. It therefore requires a mesh, unlike SPH, and it is based on standard numerical techniques for solving the Navier-Stokes equations. Ref. [19] provides a detailed description of an implementation of the method to incompressible flows. Commercial codes

such as Fluent by ANSYS and FLOW-3D by FLOW SCIENCE employ VoF for free surface modelling.

The basic idea behind the method is the addition of one equation to the classical conservation principles, which is used to track the free surface. For a liquid-gas system, let α be the liquid volume fraction defined as:

$$\alpha = \frac{V_l}{V_l + V_g} \tag{6}$$

Where V is the volume and subscripts l and g indicate the liquid and gas phase respectively for a given cell of the domain mesh. The conservation of mass in Eulerian formulation for the liquid phase can be written as:

$$\frac{\partial}{\partial t}[\alpha \rho_l] + \frac{\partial}{\partial x_j}[\alpha \rho_l V_j] = 0 \tag{7}$$

Where t is time and summation is taken over the repeated index j, which indicates spatial coordinates.

At each time step, the value of the volume fraction in each cell of the domain mesh is computed by numerical integration of equation (7) effectively advecting the interface between liquid and gas. This numerical integration implies a spatial numerical differentiation at the previous time step, and a subsequent time marching algorithm to evaluate the solution at the current time step.

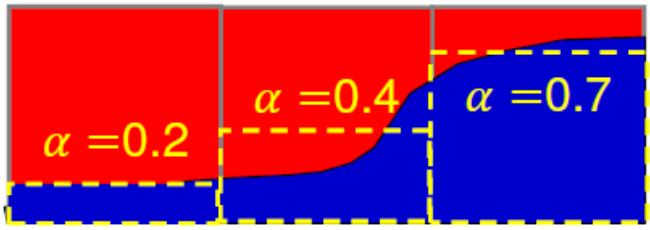

Figure 12: Volume Fraction

Any available numerical technique can then be adopted to solve the Navier-Stokes equations for the velocity, pressure and density fields in the domain, for both the liquid and the gas phases. As it is natural extension of traditional Eulerian methods, Volume of fluids can naturally cope with no-slip boundary conditions.

Following from the definition of the volume fraction given in equation (6), $\alpha = 1$ in cells filled with liquid, $\alpha = 0$ in cells filled with air and $0 < \alpha < 1$ in cells at the interface, see also Figure 12. Therefore an intrinsic characteristic of VoF is that the free surface is not defined sharply, but smeared across the volume of the cells at the interface. Adaptive mesh refinement can be performed for improved accuracy if required (ref. [20]), and it is naturally limited to cells at the interface (identified by $0 < \alpha < 1$).

4.2.1 Numerical Simulations

All results have been derived using the software Elemental™ currently being developed at the CFD research group of the University of Cape Town (with some preliminary results derived at the CSIR). For the sloshing frequency test case, already discussed in section 4.1.1, a comparison of experimental and numerical data is presented in Figure 13. Numerical results are labelled (Elemental 6k and BAE-SPH, after the software used for the simulations).

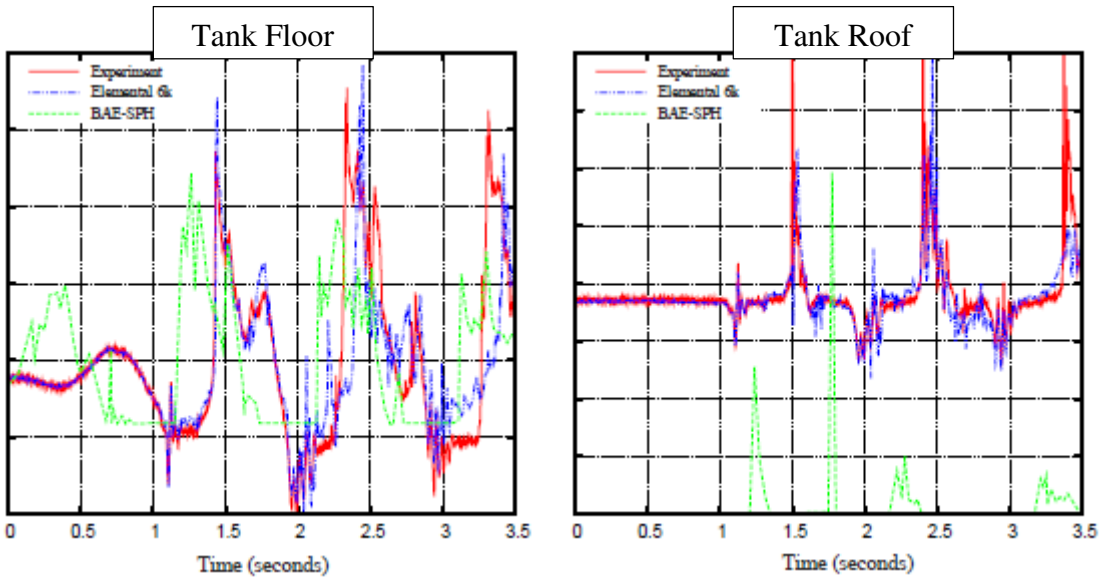

Figure 13: Sloshing Frequency – Floor and Roof Pressures

The VoF calculation is performed for the first 3.5s of the experiments using a 6000 nodes mesh, as it can be seen from the time histories the pressures on tank floor and roof are predicted with higher accuracy by VoF (Elemental™) than SPH (BAE-SPH). It should be noted that the pressures in this comparisons have been offset for hydrostatic calibration (which was not the case for the comparisons in section 4.1.1).

The increased accuracy due to the modelling of the gas phase is obvious for the tank roof, where the suction effect of the air being pulled away from the wall is captured by the numerical simulation consistently with the measurements.

At the tank bottom the VoF pressure time history is better correlated to the measurements than the SPH results, with no phase shift between numerical and experimental data. However after the second peak some discrepancies start to occur. This improvement is attributed to the oscillation damping effect of the gas phase.

Following from the experience with sloshing frequency test case (and the previous SPH validation exercise described in section 4.1), the capabilities of the VoF method in modelling the effects of the gas phase are investigated further, with particular focus to:

- The cushioning effect in vertical (perpendicular to the free surface) excitation cases
- The interaction of the liquid and gas phases with the tank roof, which causes highly non-linear behavior of the free surface, with phenomena such as wake breaking.

Therefore a test case with 75% fill level and saw-tooth type excitation is selected and modelled with Elemental™. The choice is driven by the expectation of strong interaction between of liquid, gas and tank roof. Figure 14 shows the acceleration time histories of the

input command for the shake table and the measured value from accelerometer mounted on the tank platform.

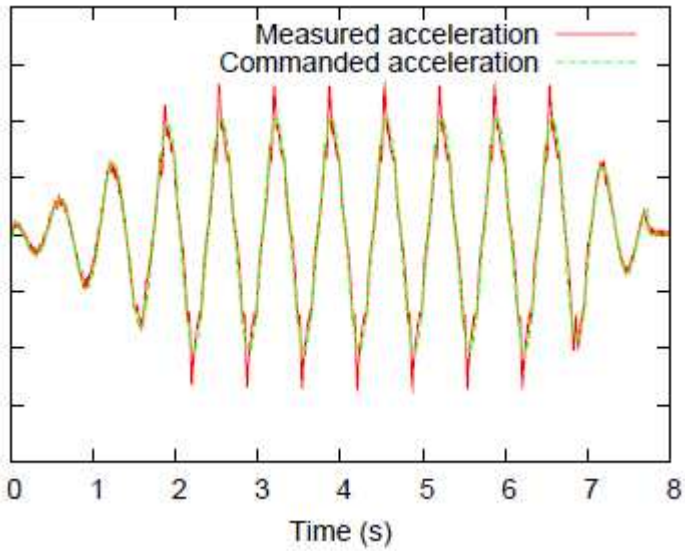

Figure 14: Vertical Saw-tooth - Accelerations

The measured acceleration exceeds the peak values of the command, due to lags in motion controller of the shake table. It is important to notice that the commanded, rather than measured, acceleration is used to drive the numerical simulations.

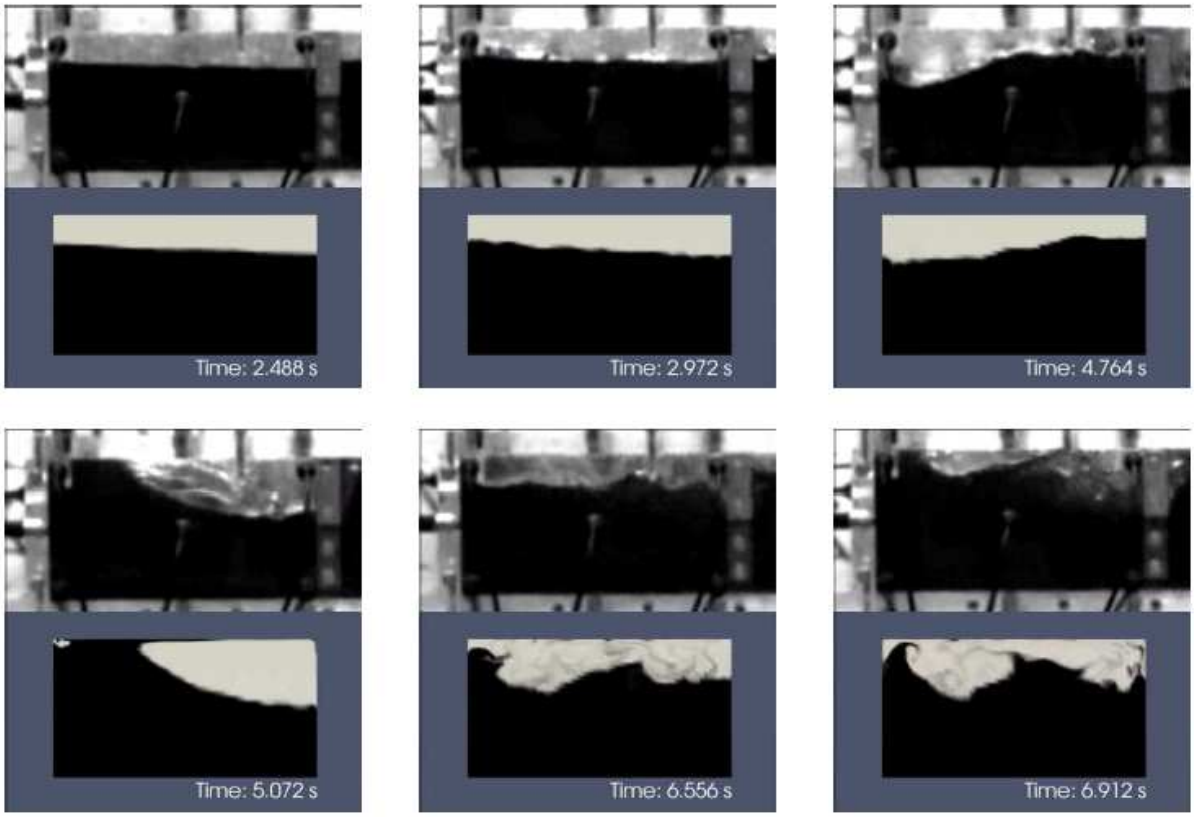

Figure 15: Vertical Saw-tooth – Flow Features

Figure 15 presents a series of snapshots in time of the VoF simulation and video recordings for the vertical saw-tooth case. Pressures time histories for the tank floor and roof are given in Figure 16.

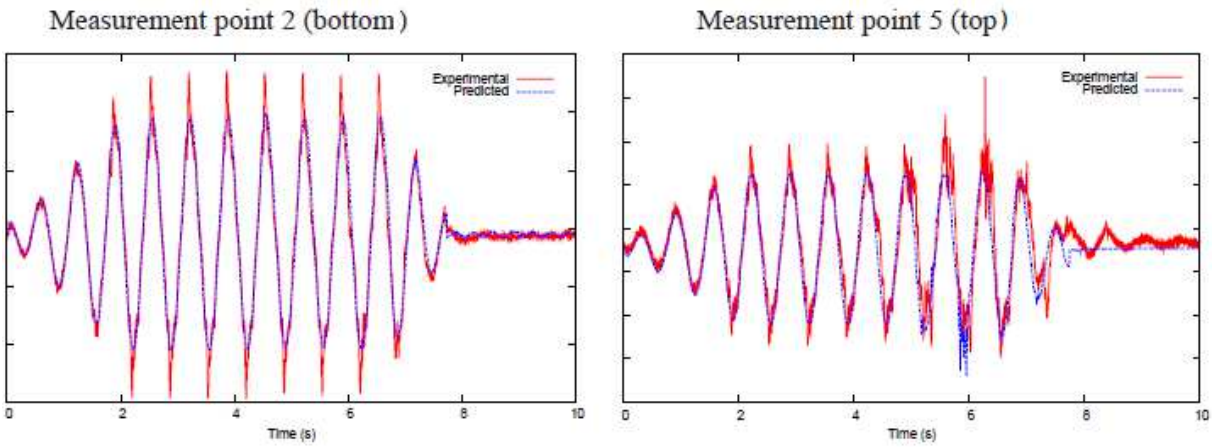

Figure 16: Vertical Saw-tooth – Floor and Roof Pressures

The flow features are well represented in the numerical prediction, particularly the interaction of the wave breaking at corner between the side and the roof of tank. The smearing of the free surface typical of the VoF method can be observed at the later stages of the simulation.

VoF pressure time histories show also very good correlation with the measured data at the tank floor and roof. The discrepancy observed in terms of peak accelerations is attributed to the commanded acceleration being used to drive the tank in Elemental^{TM} (as opposed to the measured acceleration at the shake table).

Further comparisons of experimental and numerical results for the VoF method are provided in ref. [15]. In the same reference a lateral (parallel to the free surface and perpendicular to the baffle) excitation case is also considered.

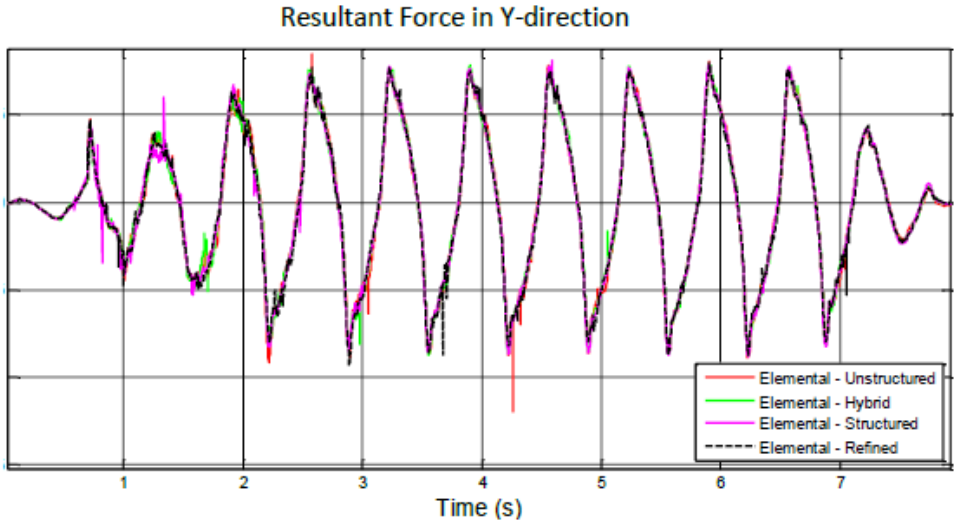

Figure 17: Lateral Saw-tooth – Resultant Force

Elemental^{TM} results are compared with experimental data in terms of net force applied to the tank. The force is derived via integration of the wall pressures. Numerical results are presented for various mesh topologies, all showing good correlation with the measured data.

Following the validation exercise, VoF is regarded as a valuable mean to understand the qualitative nature of the flow field and to accurately predict wall pressures within large aircraft fuel tanks. In fact the characteristic free surface smearing (generally regarded as a limitation for the method) does not affect significantly the interaction of liquid and gas phases with the tank boundaries. Therefore the method is chosen to derive design rules for the calculation of wall pressures.

5 FUEL TANK DESIGN RULES

The work described in this section has been performed at the University of Cape Town and is recorded in ref. [21]. The aim is to provide a reliable methodology for calculating the dynamic amplification factors of equation (2), applicable to the design conditions of large aircraft tank.

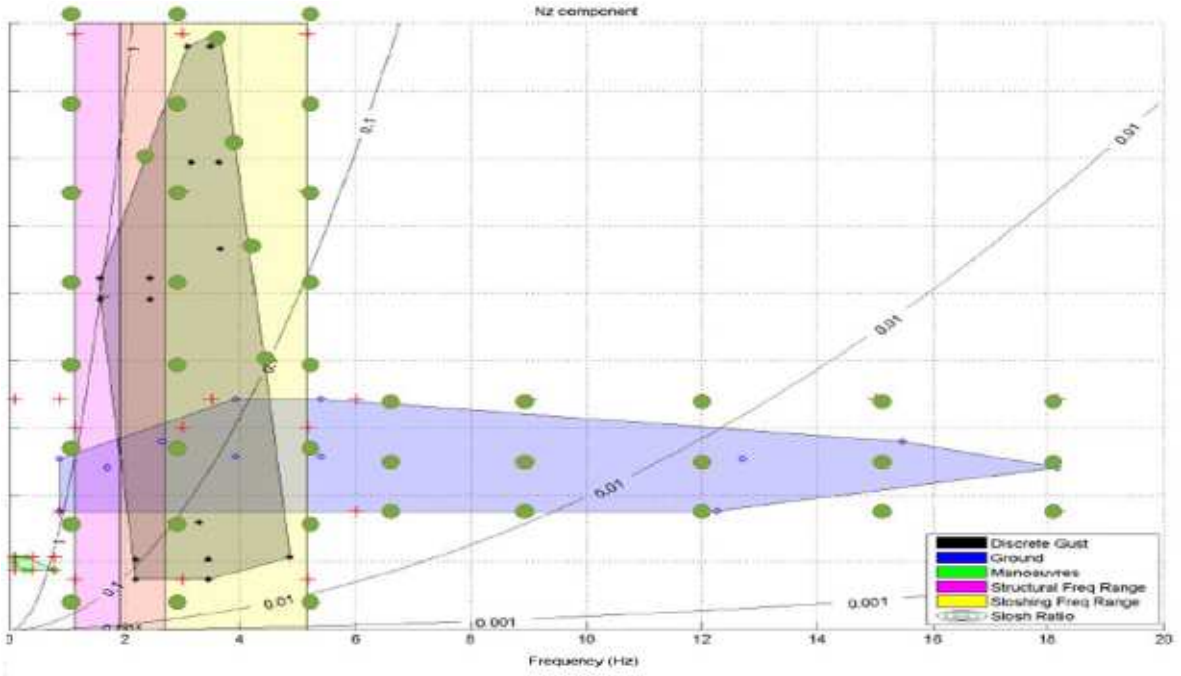

Figure 18: Tank Design Space – Acceleration Vs Frequency

The tank design space is defined in terms of accelerations and frequencies, derived from a survey of loads model results, see Figure 18 where vertical (z) accelerations are plotted against frequencies.

The different shaded areas in the plot represent different loading conditions, while the circles indicate the chosen simulation points for VoF. For each of those points:

- A sinusoidal time-varying acceleration is applied to the tank,
- Tank geometry is the same as that of the experimental tests,
- Output forces computed by Elemental^{TM} due to wall pressures are analyzed,
- A 99 percentile threshold is applied to the force time history to filter spurious numerical results,
- The calculated force is compared with analytical force from Newton's 2nd law applied to the tank mass,
- The dynamic amplification factor is derived as the ratio between the VoF calculated force and the analytical force of excitation.

Figure 19 shows an example of the procedure for a given calculation point, where a spurious numeric result is eliminated by the 99 percentile analysis.

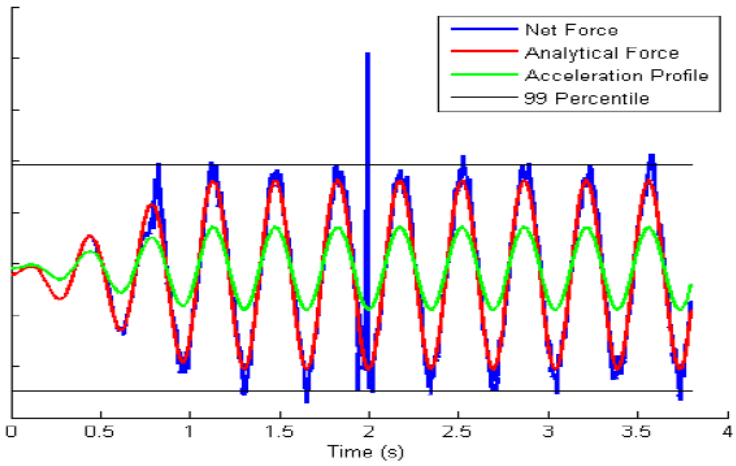

Figure 19: Derivation of Dynamic Amplification Factors

The procedure is applied to the three different fill levels: 25, 50 and 75% and all data points are subsequently used to train a Reduce Order Model (ROM) for the amplification factor as function of acceleration and frequency. As described in ref. [21] a Kriging interpolation is used to generate the model.

Results for the vertical accelerations are shown in Figure 20.

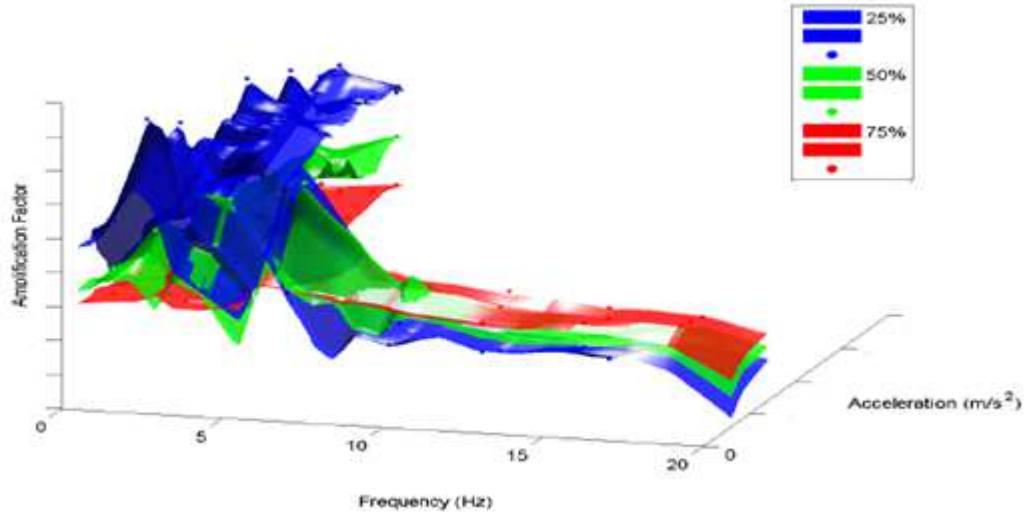

Figure 20: Amplification Factors for Vertical Accelerations

The following features are observed:

- The magnitude of the peak amplification is higher for lower fill levels.
- The peak is reached in the region of 0 – 10 Hz for all fill levels.
- At higher frequencies the factors tend asymptotically to a constant value.

The methodology can be applied to excitations in other directions, with similar results (ref. [21]). For the calculation of the fuel tank pressures is of interest to notice that as expected the calculated factors are below what previously used for design (see section 2.2).

Therefore the proposed approach offers a rational to reduce conservatism in the application of equation (2), with trivial modification to the approach currently used for industrial applications.

6 CONCLUSIONS AND FUTURE WORK

The validation and verification exercises of two numerical methods, SPH and VoF, are presented through comparisons with experimental tests.

While SPH is found capable of modelling the flow features of typical problems related to large aircraft tank design, VoF demonstrates superior capabilities in predict wall pressures.

Therefore the VoF method is successfully used to derive a set of dynamic amplification factors, less conservative then what currently in use in industry, which can be readily employed in the design process.

Current and future work would look at the derivation of "equivalent" mechanical models of the type described in [3]-[5], based on a coupled loads/VoF model. Part of the work on this subject is described in a parallel paper, ref. [22].

7 REFERENCES

[1] The 'Galileo' program, available on line at the Airbus Defense and Space website: https://airbusdefenceandspace.com/our-portfolio/space-systems/satellite-navigation/

[2] 'Ariane 6 configuration', available on line at the Airbus-Safran Launcher website: https://www.airbusafran-launchers.com/en/universe_theme/ariane-6-configurations-2/

[3] H. Norman Abramson, 'The Dynamic Behaviour of Liquids in Moving Containers', NACA SP-106, Washington D.C, 1966.

[4] Franklin T. Dodge, 'The New Dynamic Behaviour of Liquids in Moving Containers', Southwest Research Institute, San Antonio Texas.

[5] Raouf A. Ibrahim, 'Liquid Sloshing Dynamics Theory and Applications', Cambridge University Press, Cambridge, 2005.

[6] 'C295', available on line at the Airbus Defense and Space website: https://airbusdefenceandspace.com/our-portfolio/military-aircraft/c295/

[7] Robert Banim, et al., 'Smoothed Particle Hydrodynamics Simulation of Fuel Tank Sloshing', 25th International Congress of Aeronautical Sciences.

[8] Robert Banim, 'Some Industrial SPH Applications Undertaken at the BAE Systems Advanced Technology Centre', SPHERIC Conference Paper 2007

[9] Arnaud Malan and Oliver Oxtoby, 'A Parallel Free-Surface-Modelling Technology for Application to Aircraft Fuel Sloshing', Lisbon, ECCOMAS CFD – Fifth European Conference on Computational Fluid Dynamics, Lisbon 14-17 June 2010.

[10] A.G.B Mowat., et al., 'An Algebraic Multigrid Solution Strategy for Efficient Solution of Free-Surface Flows', International Journal for Numerical Methods in Heat and Fluid Flow, Volume 26(3-4), pp. 1172-1186 (2016).

[11] European Aviation Safety Agency, 'Certification Specifications and Acceptable Means of Compliance for Large Aeroplanes', CS-25 Amendment 19, 12th May 2017.

[12] Francesco Gambioli, 'Fuel loads in Large Civil Airplanes', Proc. 4th Spheric Workshop, Nantes, France, 247, 2009.

[13] R.L.Bass, et al, ‘Modeling Criteria for Scaled LNG Sloshing Experiments’, Transactions of the ASME Journal of Fluids Engineering, Vol 107, June 1985.

[14] Rayand Ramlal, ‘Similitude and Experimental Assessment for Fuel Sloshing in Aircraft’, University of CapeTown Msc Thesis, 2013.

[15] Niran Ilangakoon, ‘On the Detailed Modelling and Analysis of Liquid Sloshing and its Effects in a Rectangular Baffled Tank’, University of CapeTown Msc Thesis, 2013.

[16] G R Liu, M B Liu, ‘Smooth Particle Hydrodynamics, A Meshfree Particle Method’, World Scientific Publishing Co. Pte. Ltd., 2003.

[17] A. Di Monaco, et al A semi-analytic approach for SPH modelling of solid, Proc. 4th Spheric Workshop, Nantes, France, 247, 2009.

[18] Richard Mant, ‘Airbus Fuel Systems Simulation and Validation’, BAE-Systems report to Airbus, TES105127 issue2, January 2010.

[19] M. D. Torrey, et al., ‘NASA-VOF2D, a Computer Program for Incompressible Flows with Free Surfaces’, Los Alamos National Laboratory, 1985.

[20] A. E. J. Bogaers, S. Kok, A. G. Malan, 'Highly Efficient Optimization Mesh Movement Method Based on Proper Orthogonal Decomposition', Int. J. of Numerical Methods in Engineering, Vol. 86, Issue 8, 27th May 2011, Pages 935-952.

[21] Byron Sykes, ‘Charactering Fuel Sloshing Loads in Aircraft, University of CapeTown Msc Thesis, 2014.

[22] Javon Farao, ‘Towards a Non-Linear Full Aircraft Model For Passenger Aircraft Loads Calculations’, International Forum Aeroelasticity and Structural Dynamics, Como, Italy, June 2017.

ACKNOWLEDGMENTS

The authors would like to thank:

- BAE-Systems and the CSIR for their work under contract by Airbus, in the person of Richard Mant, Robert Banin, Chris Constantinou and Dr.Oliver Oxtoby.
- All the students at the University of Cape Town for their innovative and inspired work, in particular: Rayand Ramlal, Niran Ilangakoon, Byron Sykes and Javon Farao.
- The National Aerospace Centre (NAC) of the University of Witwatersrand, Johannesburg as well as South African Research Chair (SARChI) in Industrial CFD for co-funding this work. SARChI is funded by the Department of Science and Technology (DST) and the National Research Foundation (NRF).
- Last, but not least, their wives for their patience and relentless support.

COPYRIGHT STATEMENT